GAS SIDE HEAT TRANSFER - 2-D FLOW

Ronald York
Detroit Diesel Allison
Indianapolis, Indiana

The work reported herein is being performed under NASA contract NAS 3-22761 entitled, "Development of Analytical Techniques for Improved Prediction of Local Gas-to-Blade Heat Transfer". The objectives of the program were to assess the capability of currently available modeling techniques to predict airfoil surface heat transfer distributions in a 2-D flow field, acquire experimental data as required for model verification, and to make and verify improvements in the analytical models. Chart No. 1 summarizes the program task structure.

Two data sets, Turner[1] and Lander[2], were selected from the literature for use in evaluating models in Task I. Two additional airfoils were chosen for cascade testing under this contract. These airfoils, the Mark II and C3X, are representative of highly loaded, low solidity airfoils currently being designed. Cross sections of the four airfoils and the grid used to make inviscid flow predictions for each airfoil are shown in Chart No. 2. Note the significant variation in airfoil geometry. This variation is intended to provide a significant test of the analytical models. Predicted surface pressure distributions for the four airfoils are shown in Chart No. 3.

The two heat transfer cascades that were operated under Task II were run in the Detroit Diesel Allison Aerothermodynamic Cascade Facility (ACF). The facility, described in Chart No. 4, provides the capability of obtaining both heat transfer and aerodynamic measurements at simulated engine conditions. The method employed in the facility to obtain airfoil surface heat transfer measurements is shown schematically in Chart No. 5. Basically, the exterior of the airfoil is instrumented with grooved surface thermocouples with this data serving as the exterior boundary condition input to a finite element analysis. The internal boundary conditions are calculated heat transfer coefficients in the internal cooling holes. These values are calculated from measurements of the coolant temperature, pressure and flowrate. A photo of the three-vane, 2-D C3X cascade is shown in Chart No. 6. The vane surface thermocouples appear as lines on the surface. This center airfoil also contains static pressure taps, thus permitting simultaneous measurement of the surface pressure and heat transfer distributions.

The test matrix over which both cascades were operated is shown in Chart No. 7. Data was obtained at two exit Mach numbers, 0.9 and 1.05, and over a range of exit Reynolds numbers from $1.5X10^6$ to $2.5X10^6$. The inlet turbulence intensity and wall-to-gas temperature ratio were also varied. Chart No. 8 shows typical data from the Mark II cascade. The effect of variation in Reynolds number is clearly evident. The heat transfer measurement technique is capable of detecting the rapid increase in heat transfer caused by separation and reattachment on the suction surface. This separation is a result of the large adverse pressure gradient on the Mark II airfoil. Similar data for the C3X cascade is shown in Chart No. 9. Here the suction surface demonstrates transition and the effect of Reynolds number on the location of the start of transition can be clearly seen. Chart No. 10 illustrates the Mach number effects on heat transfer in the Mark II cascade. As would be expected the Mach number effects are seen only on the suction surface in the region where the Mach number affects the pressure distribution. A summary of the results found with the Mark II and C3X cascades is shown in Chart No. 11.

Charts 12-22 present some preliminary results of the analytical work being done using 2-D boundary layer theory for establishing an acceptable approach for predicting gas turbine airfoil heat transfer over a wide range of operating conditions and geometries. Starting with the STAN5 mixing length (ML) theory turbulence modeling evaluated in Task I, Task III efforts have been directed towards supplying systematic boundary and initial conditions and structuring a realistic gas turbine airfoil environment ML turbulence model which reflects free-stream turbulence, transition, curvature, pressure gradient, etc.

The importance of specifying realistic velocity (pressure) boundary conditions over the entire airfoil surface and generating appropriate initial velocity and thermal profiles is often understated because of more noticeable inadequacies in turbulence modeling. Specifying the correct velocity boundary conditions is very important since the Reynolds number and pressure gradient play important roles physically and in the development of turbulence and/or transition models. Specification of correct initial thermal profiles near the stagnation point are essential to accurately obtain leading edge heat loads. Boundary conditions for all boundary layer calculations are currently being obtained from the inviscid blade-to-blade Euler solver developed by Delaney at DDA. The ability of this method to accurately predict the inviscid pressure distribution is illustrated by Chart 12 for the Mark II airfoil. In addition, because the Delaney method uses a body-centered coordinate system (example shown on Chart 2), it provides excellent resolution of the velocity distribution from the stagnation point to the trailing edge. This ability to resolve the velocity field in the near-stagnation-point region has provided much insight and has guided modeling efforts aimed at generating initial velocity and thermal profiles. Initial profiles are generated from boundary layer similarity solutions assuming stagnation flow, i.e, Euler number equal to unity. Based on the work of Miyazaki and Sparrow[3], who extended the laminar similarity solution concept to include the effects of free-stream turbulence for flow normal to a cylinder, a more general system of equations and turbulence model was developed at DDA to reflect the differences between stagnation flow on an airfoil from that on a circular cylinder. These changes are summarized on Chart 13. Changes include recasting the equations in compressible form and directly using the near-stagnation-point pressure-gradient calculated from the inviscid analysis rather than assuming an isolated cylinder value. Also, the Miyazaki and Sparrow turbulence model was generalized to reflect variable stagnation point pressure gradient. The results of this approach for predicting airfoil stagnation point heat transfer are shown in Chart 14. The open symbols are predictions using the Miyazaki and Sparrow turbulence model and the solid symbols represent predictions using DDA's generalized form. As can be seen, the present scheme is capable, in most instances, of predicting stagnation point heat transfer within ±10% of the experimental mean. These results are encouraging because the data span a wide range of turbulence levels (0.45 - 18%) and geometries. These results are a direct outcome of relaxing the cylinder-in-crossflow assumption, and properly modeling the near-stagnation-point velocity field using the body-centered coordinate system Euler solver.

The remaining charts 15-22, highlight progress towards developing a realistic ML turbulence model for a 2-D finite difference boundary layer code. Chart 15 presents the analytical form of the effective viscosity (μ_{eff}) being studied. Note the presence of two turbulent terms, μ_t and μ_{TU}. The principle difference in the two terms is the velocity scale assumed. The additional term is included to account for the significant effects of free-stream turbulence on heat transfer for nominally laminar boundary layers observed on turbine airfoils. The intermittency functions γ_t and γ_{TU} incorporate information regarding transition behavior. Besides evaluating promising published μ_{eff} models, a significant inhouse effort is in progress aimed at taking advantage of the large amount of data collected within this program. At the present time, the majority of the modeling effort has gone into structuring a suitable model for the turbulence viscosity term μ_{TU}. As contrasted on Chart 15, a major difference between Task I prediction methodology and the Task III concept is the inclusion of μ_{TU}. The general functional form for μ_{TU}, currently being explored, is shown in Chart 15. Although the exact form is not finalized, one key feature is that the model is compatible with the similarity solution stagnation flow analysis in that the effects of free-stream turbulence incorporated in the function f is carried forward into the surface boundary layer computation.

The last charts (15-22) present heat transfer predictions compared to experimental data from four different airfoil heat transfer experiments. Predictions are shown using the original STAN5 mixing length turbulence model with the transition Reynolds number set to 250, and the current Task III concept turbulence model for μ_{TU}. For the later predictions, the term γ_t was set to zero to allow only the influence of μ_{TU} to be seen in the μ_{eff} definition. Attention should be directed to the pressure surface predictions where the effects of free-stream turbulence are most dominant and therefore, the modeling of μ_{TU} more important.

Predictions for the Mark II airfoil, for one Reynolds number level, using the Task I and present Task III approaches are shown in Chart 16. Of particular interest is the better pressure surface prediction obtained using the additional "turbulence" viscosity term over a standard laminar/transitional/turbulent approach. Suction surface predictions were only possible up to the location of the shock, where the boundary layer code reached a separation condition. Chart 17 shows Task III concept predictions for the Mark II airfoil at three different exit Reynolds number levels and indicate, at least on the pressure surface, that both trends and levels are reasonably well predicted.

Chart 18 shows predictions for the C3X airfoil at a single exit Reynolds number and again there is a significant improvement in pressure surface prediction. The suction surface prediction is in poor agreement beyond the transition point, but as mentioned earlier transition modeling has not yet been addressed in the Task III predictions since $\gamma_t = 0$.

Charts 19 and 20 show predictions for the Turner airfoil and serve to illustrate the influence of free-stream turbulence. Since the original STAN5 ML turbulence model does not model free-stream turbulence effects directly, only one prediction is possible for the three different experiments as shown on Chart 19. In contrast, Chart 20 shows the effects of free-stream turbulence are adequately modeled on the pressure surface using the current μ_{TU} concept, but the suction surface predictions only indicate proper trends not levels.

Finally, predictions for the Lander airfoil are presented in Charts 21 and 22 respectively. It is clear that substantial predictive improvement can be attributed to the use of the turbulence viscosity although still, predictions beyond the indicated transition zone are not well modeled with this approach.

In conclusion, to date significant progress has been made in advancing the idea of establishing a unified approach for predicting airfoil heat transfer for a wide range of operating conditions and geometries. Preliminary results are encouraging and further ML turbulence modeling ideas will be explored in the remaining phase of the program, primarily concentrating on transition behavior through γ_t and γ_{TU} modeling.

REFERENCES

(1) A. B. Turner, "Local Heat Transfer Measurements on a Gas Turbine Blade", Jour. of Mechanical Engng. Sciences, Vol. 13, 1971, pp. 1-12.

(2) R. D. Lander, "Effect of Free-Stream Turbulence on the Heat Transfer to Turbine Airfoils", Tech. Rept. AFAPL-TR-69-70, Air Force Systems Command, Sept. 1969.

(3) H. Miyazaki and E. M. Sparrow, "Analysis of Effects of Free-Stream Turbulence on Heat Transfer and Skin Friction", Jour. of Heat Transfer, Trans. ASME, Vol. 99, 1977, pp. 614-419.

LIST OF SYMBOLS

C Chapman-Rubesin parameter, $\rho\mu/\rho_e \mu_e$

F Similarity function related to velocity

f Empirical function in turbulence viscosity definition

G Similarity function related to temperature or enthalpy

g Empirical function in turbulence viscosity definition

H Shape factor

ℓ Length scale in mixing length hypothesis

M Mach number

p Pressure

Pr Prandtl number

Re Reynolds number

T Temperature

u Velocity

X Coordinate in streamwise direction

y Coordinate normal to streamwise direction

GREEK

β Euler number

γ Intermittency function, or specific heat ratio when unsubscripted

δ Boundary layer thickness

ϵ Eddy viscosity

Λ Pressure gradient parameter

μ Molecular viscosity

ν Kinematic viscosity

ρ Density

SUBSCRIPTS

D Refers to leading edge diameter or twice radius of curvature

e Refers to outer edge of boundary layer

eff Effective quantity

m Refers to momentum

t Refers to turbulent

tr Refers to transition

TU Refers to turbulence intensity

θ Momentum thickness

∞ Upstream quantity

SUPERSCRIPTS

' Refers to fluctuating quantity

OTHER

< > Refers to root-mean-square (RMS) value

|| Absolute value

Detroit Diesel Allison
Division of General Motors Corporation
Indianapolis Indiana

NAS 3-22761
GAS SIDE HEAT TRANSFER - 2-D FLOW

DATE
CHART NO. 1

PROGRAM OBJECTIVE AND TASK STRUCTURE

OBJECTIVE: THE DEVELOPMENT OF ANALYTICAL TECHNIQUES FOR IMPROVED PREDICTION OF LOCAL GAS-TO-BLADE HEAT TRANSFER COEFFICIENTS. (NON-FILM COOLED)

TASK I : CHARACTERIZE THE PREDICTIVE PERFORMANCE OF EXISTING METHODS USING AVAILABLE EXPERIMENTAL DATA.

TASK II : PERFORM AIRFOIL HEAT TRANSFER EXPERIMENTS TO FURTHER SUPPLEMENT THE DATA BASE AND IDENTIFY PHENOMENA OF INTEREST.

TASK III: SUGGEST, IMPLEMENT, AND VERIFY ANALYTICAL METHOD CHANGES BASED ON AVAILABLE KNOWLEDGE AND TASK I AND II FINDINGS.

TASK IV: REPORTING & PROGRAM ADMINISTRATION.

FORM 8040(REV. 5-75)

Detroit Diesel Allison
Division of General Motors Corporation
Indianapolis Indiana

NAS 3-22761
GAS SIDE HEAT TRANSFER - 2-D FLOW

DATE
CHART NO. 2

AIRFOIL PROFILES AND GRIDS FOR INVISCID SOLUTIONS

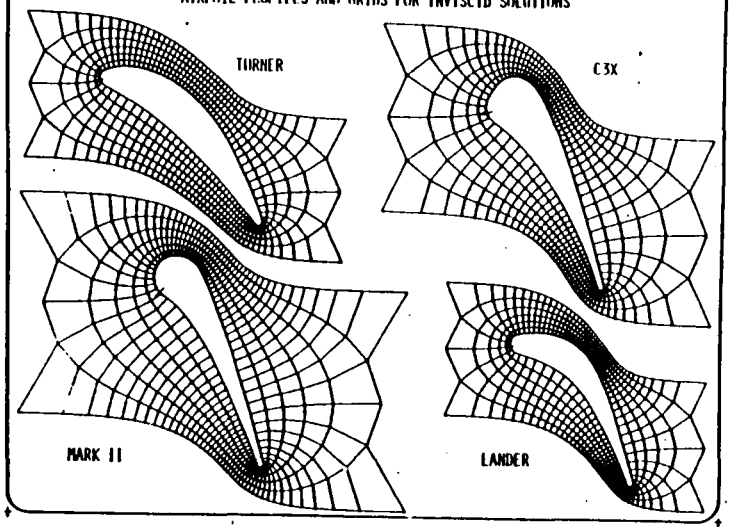

FORM 8040(REV. 5-75)

Detroit Diesel Allison
Division of General Motors Corporation
Indianapolis Indiana

NAS 3-22761
GAS SIDE HEAT TRANSFER - 2-D FLOW

DATE
CHART NO. 3

AIRFOIL PREDICTED SURFACE PRESSURE DISTRIBUTION

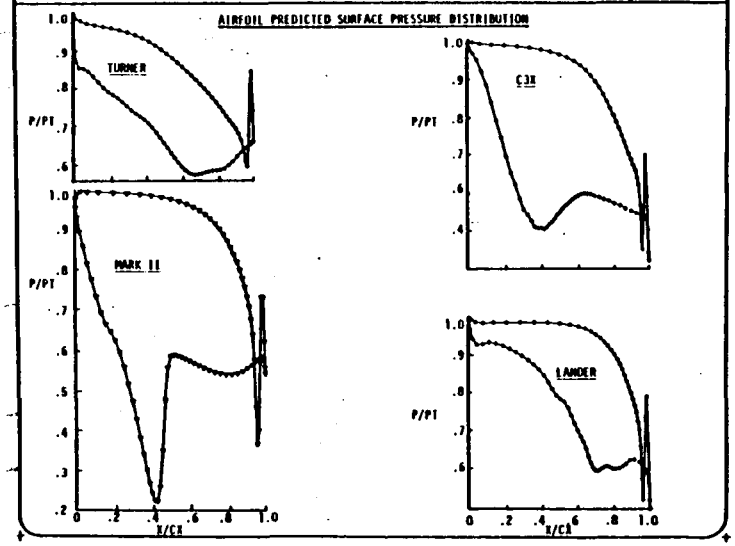

FORM 8040(REV. 5-75)

Detroit Diesel Allison
Division of General Motors Corporation
Indianapolis Indiana

NAS 3-22761
GAS SIDE HEAT TRANSFER - 2-D FLOW

DATE
CHART NO. 4

DDA AEROTHERMODYNAMIC CASCADE FACILITY

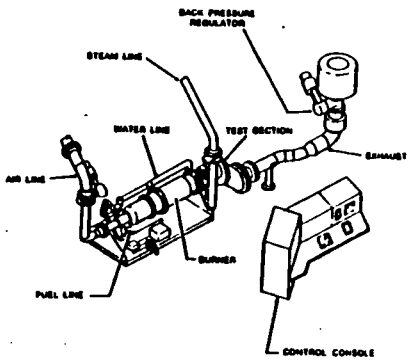

OPERATIONAL PHILOSOPHY

- TWO-DIMENSIONAL LINEAR CASCADE
- PROVIDES HEAT TRANSFER AND AERODYNAMIC DATA SIMULTANEOUSLY
- OPERATED AT SIMULATED ENGINE CONDITIONS
  - REDUCED TEMPERATURE
  - REDUCED PRESSURE
  - SCALED-UP AIRFOIL GEOMETRY
  - HIGH FREESTREAM TURBULENCE
- WIDE OPERATING RANGE
  - REYNOLDS NUMBER CONTROL
  - EXIT MACH NUMBER CONTROL
  - WALL-TO-GAS TEMPERATURE RATIO CONTROL
  - INLET TURBULENCE INTENSITY CONTROL
- HIGH DENSITY INSTRUMENTATION
  - UP TO 300 TEMPERATURES
  - UP TO 288 PRESSURES
- DEDICATED FACILITY COMPUTER
  - COMPUTER CONTROLLED DATA ACQUISITION
  - ONLINE DATA ANALYSIS

OPERATIONAL SPECIFICATIONS

AIR SUPPLY	9.5 LB/SEC AT 105 PSIA OR 5.0 LBM/SEC AT 245 PSIA
INLET PRESSURE	20 PSIA TO 245 PSIA
STAGNATION TEMPERATURE	400°F TO 3200°F
PRIMARY FUEL	NATURAL GAS

Detroit Diesel Allison
Division of General Motors Corporation
Indianapolis, Indiana

NAS 3-22761
GAS SIDE HEAT TRANSFER - 2-D FLOW

DATE
CHART NO. 5

HEAT TRANSFER MEASUREMENT TECHNIQUE

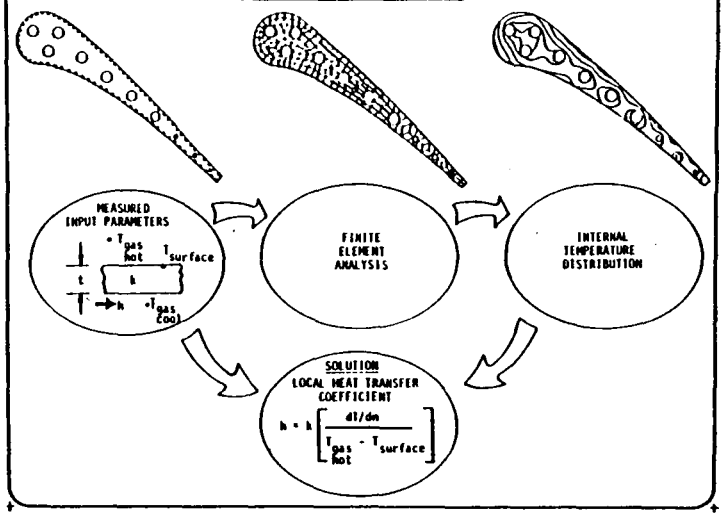

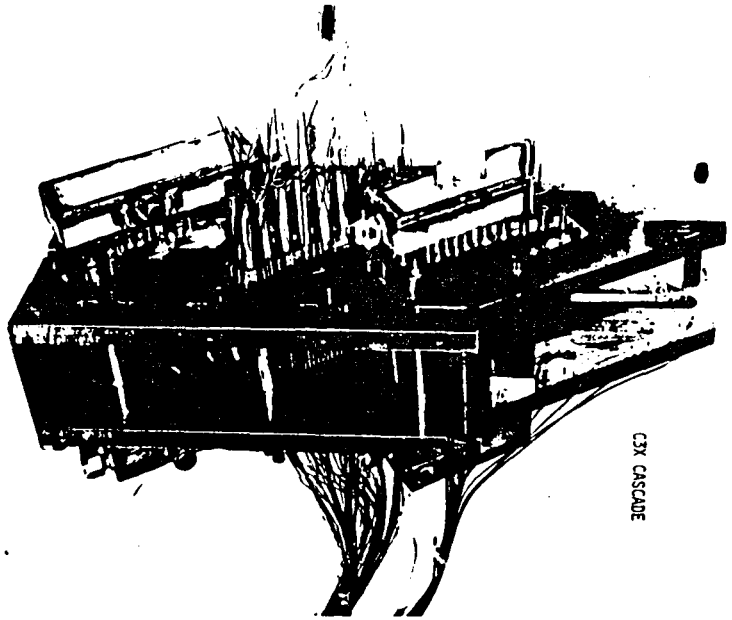

C3X CASCADE

CHART NO. 6

Detroit Diesel Allison
Division of General Motors Corporation
Indianapolis, Indiana

NAS 3-22761
GAS SIDE HEAT TRANSFER - 2-D FLOW

DATE
CHART NO. 7

MARK II AND C3X TEST MATRIX

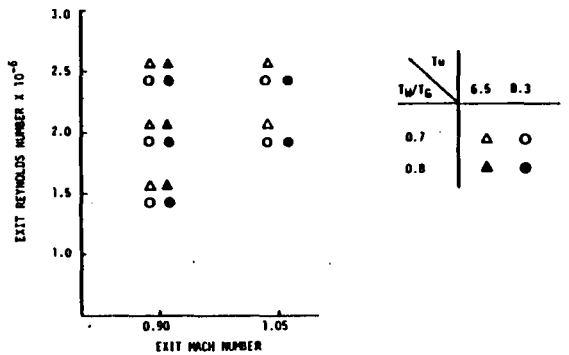

T_W/T_G \ Tu	6.5	8.3
0.7	△	○
0.8	▲	●

Detroit Diesel Allison
Division of General Motors Corporation
Indianapolis, Indiana

NAS 3-22761
GAS SIDE HEAT TRANSFER - 2-D FLOW

DATE
CHART NO. 8

REYNOLDS NUMBER EFFECT ON MARK II HEAT TRANSFER

NOMINAL RUN CONDITIONS
M_2 = 0.89
TW/T_G = 0.82
Tu = 8.3%

EXIT REYNOLDS NUMBER
▲ 1.54×10^6
■ 1.95×10^6
▼ 2.52×10^6

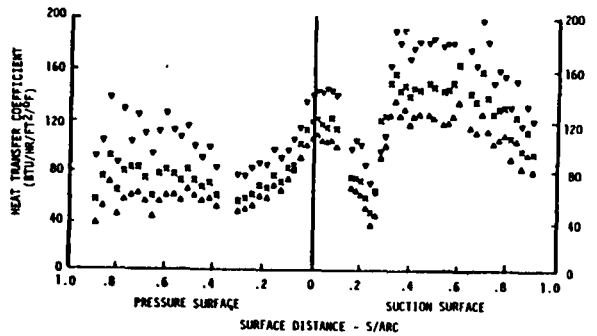

Detroit Diesel Allison
Division of General Motors Corporation
Indianapolis, Indiana

NAS 3-22761
GAS SIDE HEAT TRANSFER - 2-D FLOW

DATE
CHART NO. 9

REYNOLDS NUMBER EFFECT ON C3X HEAT TRANSFER

NOMINAL RUN CONDITIONS
M_2 = 0.90
T_W/T_G = 0.81
Tu = 6.5%

EXIT REYNOLDS NUMBER
+ 1.51×10^6
□ 1.96×10^6
◇ 2.49×10^6

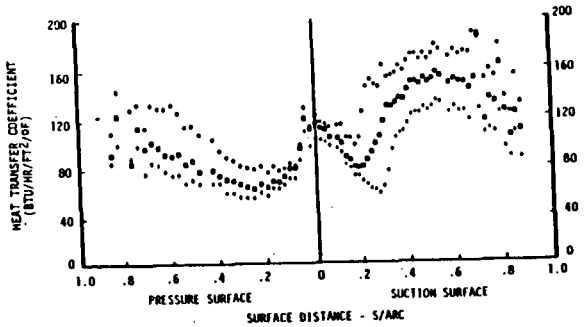

Detroit Diesel Allison
Division of General Motors Corporation
Indianapolis, Indiana

NAS 3-22761
GAS SIDE HEAT TRANSFER - 2-D FLOW

DATE
CHART NO. 10

MACH NUMBER EFFECT ON MARK II HEAT TRANSFER

NOMINAL RUN CONDITIONS
R_{e_2} = 2.0×10^6
T_W/T_G = 0.70
Tu = 6.5%

EXIT MACH NUMBER
+ 0.89
□ 1.04

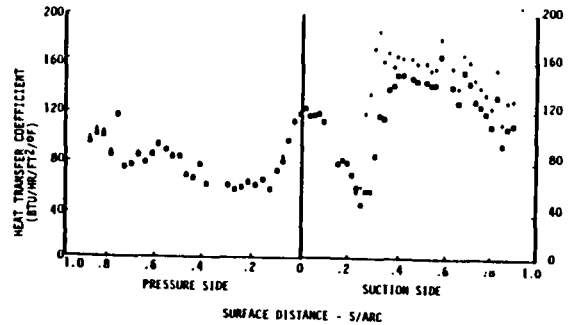

Detroit Diesel Allison
Division of General Motors Corporation
Indianapolis, Indiana

NAS 3-22761
GAS SIDE HEAT TRANSFER - 2-D FLOW

DATE
CHART NO. 11

SUMMARY OF EXPERIMENTAL RESULTS

- SUCTION SURFACE PRESSURE DISTRIBUTIONS REFLECT DIFFERENCES IN AIRFOILS
- SIMILAR PRESSURE SURFACES EXHIBIT SIMILAR HEAT TRANSFER CHARACTERISTICS
- MACH NUMBER EFFECTS ON HEAT TRANSFER DISTRIBUTION PARALLEL MACH NUMBER EFFECTS ON STATIC PRESSURE DISTRIBUTION
- MARK II SUCTION SURFACE HEAT TRANSFER DISTRIBUTIONS INDICATE SEPARATION/REATTACHMENT
- C3X SUCTION SURFACE HEAT TRANSFER DISTRIBUTIONS INDICATE TRANSITIONAL BEHAVIOR
- REYNOLDS NUMBER HAS STRONG INFLUENCE ON HEAT TRANSFER LEVEL FOR BOTH AIRFOILS
- T_W/T_G AND TURBULENCE EFFECTS ARE SMALL BUT SYSTEMATIC

Detroit Diesel Allison
Division of General Motors Corporation
Indianapolis, Indiana

NAS 3-22761
GAS SIDE HEAT TRANSFER - 2-D FLOW

DATE
CHART NO. 12

MARK II PRESSURE DISTRIBUTION

M_2 = 0.90
RUN 43

△ MEASURED
—— DELANEY PREDICTION

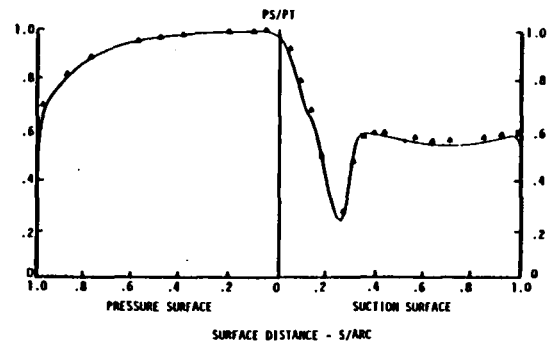

Detroit Diesel Allison
Division of General Motors Corporation
Indianapolis, Indiana

NAS 3-22761
GAS SIDE HEAT TRANSFER - 2-D FLOW

DATE

CHART NO. 13

EXTENDED SIMILARITY SOLUTION

$$\left[C\left(1+\underset{①}{\frac{\epsilon_m}{\nu}}\right)F''\right]' + FF'' + \beta\left[G-(F')^2\right] = 0 \quad \text{- MOMENTUM}$$

$$\left[C\left(\frac{1}{Pr}+\underset{②}{\frac{1}{Pr_t}\frac{\epsilon_m}{\nu}}\right)G'\right]' + FG' = -C(\gamma-1)M^2(F'')^2 \quad \text{- ENERGY}$$

- TERMS ① AND ② COMPRISE TURBULENT EXTENSION OF COMPRESSIBLE BOUNDARY LAYER SIMILARITY SOLUTION. (MIYAZAKI AND SPARROW 1977)
- ϵ_m IS MODELED USING MIXING LENGTH THEORY TO ACCOUNT FOR FREE-STREAM TURBULENCE AND PRESSURE GRADIENT EFFECTS.

$$\epsilon_m = 2.2\ell\langle u'\rangle\frac{\gamma}{\delta} \quad \text{-MIYAZAKI AND SPARROW}$$

$$\epsilon_m = f\left(Re_D/\sqrt{Re_D},\ \frac{dP}{dx}\Big|_{x=0}\right)\ell\langle u'\rangle\frac{\gamma}{\delta} \quad \text{-DDA GENERALIZED FORM}$$

- INITIAL PROFILES FOR STARTING BOUNDARY LAYER ANALYSIS ARE OBTAINED BY NOTING THAT:

$$T(y) = G$$
$$u(y) = F'$$

Detroit Diesel Allison
Division of General Motors Corporation
Indianapolis, Indiana

NAS 3-22761
GAS SIDE HEAT TRANSFER - 2-D FLOW

DATE

CHART NO. 14

STAGNATION POINT HEAT TRANSFER

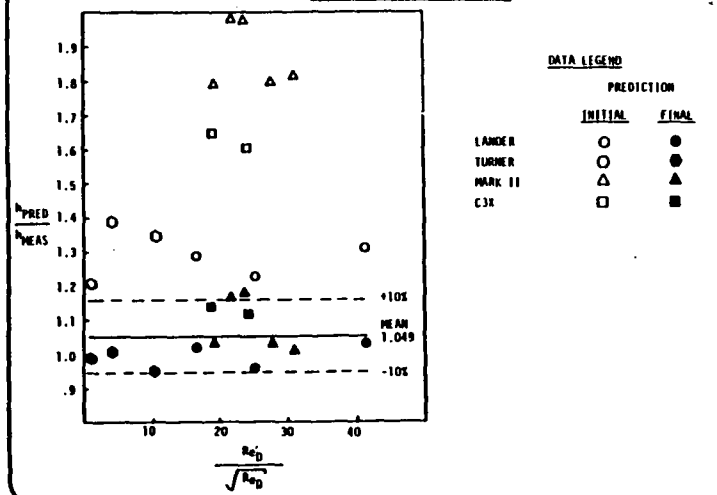

Detroit Diesel Allison
Division of General Motors Corporation
Indianapolis, Indiana

NAS 3-22761
GAS SIDE HEAT TRANSFER - 2-D FLOW

DATE

CHART NO. 15

EFFECTIVE VISCOSITY FORMULATION

$$\mu_{eff} = \mu + \gamma_t\mu_t + \gamma_{TU}\mu_{TU}$$

μ = MOLECULAR VISCOSITY

$\mu_t = \rho\ell^2\left|\frac{\partial u}{\partial y}\right|$ (TURBULENT VISCOSITY)

$\mu_{TU} = \rho\ell\langle u'\rangle$ ("TURBULENCE" VISCOSITY)

γ_t, γ_{TU} = INTERMITTENCY FUNCTIONS REFLECTING TRANSITIONAL BEHAVIOR

$$\left[0 \le \gamma_t, \gamma_{TU} \le 1\right]$$

TASK I COMPUTATIONS

STAN5 - CRAWFORD AND KAYS (1972)
MIXING LENGTH THEORY, i.e.:

- $\gamma_{TU} = 0$
- $\gamma_t = \begin{cases} 0, & Re_\theta < Re_{\theta_{tr}} \\ 1, & Re_\theta > 2\,Re_{\theta_{tr}} \end{cases}$
- $\mu_t = \rho\ell^2\left|\frac{\partial u}{\partial y}\right|$
- μ_{TU} (NOT MODELED)

TASK III MODELING CONCEPTS

- $\gamma_{TU} = \begin{cases} 1, & Re_\theta < Re_{\theta_{tr}} \\ ?, & Re_\theta > Re_{\theta_{tr}} \end{cases}$
- $\gamma_t = \begin{cases} 0, & Re_\theta < Re_{\theta_{tr}} \\ 1, & Re_\theta > ?\cdot Re_{\theta_{tr}} \end{cases}$
- $\mu_t = \rho\ell^2\left|\frac{\partial u}{\partial y}\right|$
- $\mu_{TU} = \left[f(Re_D/\sqrt{Re_D},\ \frac{dP}{dx}\Big|_{x=0}) + g(Re, H, A, \ldots)\right]\cdot \mu\ell\langle u'\rangle$

Detroit Diesel Allison
Division of General Motors Corporation
Indianapolis, Indiana

NAS 3-22761
GAS SIDE HEAT TRANSFER - 2-D FLOW

DATE

CHART NO. 16

MARK II HEAT TRANSFER DISTRIBUTION

$M_2 = 0.90$
$T_w/T_G = 0.69$
$T_u = 6.5\%$

+ RUN 43 DATA
——— TASK I PREDICTION
- - - - TASK III PREDICTION

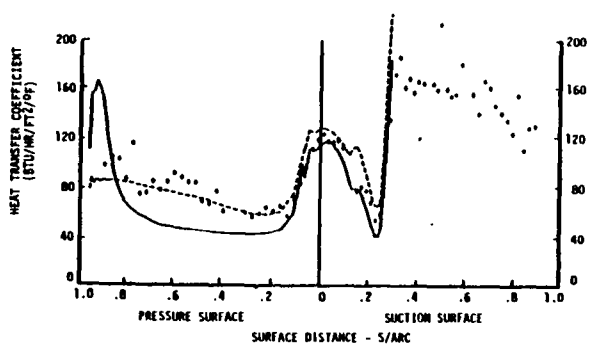

Detroit Diesel Allison
Division of General Motors Corporation
Indianapolis, Indiana

NAS 3-22761
GAS SIDE HEAT TRANSFER - 2-D FLOW

DATE
CHART NO. 17

REYNOLDS NUMBER EFFECT ON MARK II HEAT TRANSFER DISTRIBUTION

M_2 = 0.90
T_w/T_G = 0.70
Tu = 6.5%

Re_2	DATA	TASK III PREDICTION
1.5×10^6	+	———
2.0×10^6	⊡	- - - - -
2.5×10^6	♦	—·—·—

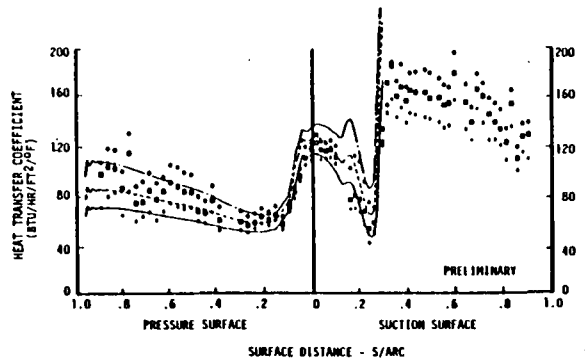

SURFACE DISTANCE - S/ARC

Detroit Diesel Allison
Division of General Motors Corporation
Indianapolis, Indiana

NAS 3-22761
GAS SIDE HEAT TRANSFER - 2-D FLOW

DATE
CHART NO. 18

C3X HEAT TRANSFER DISTRIBUTION

M_2 = 0.90
T_w/T_G = 0.72
Tu = 6.5%

+ RUN 108 DATA
——— TASK I PREDICTION
- - - - TASK III PREDICTION

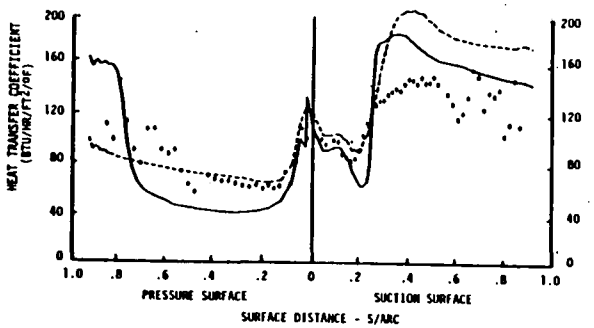

SURFACE DISTANCE - S/ARC

Detroit Diesel Allison
Division of General Motors Corporation
Indianapolis, Indiana

NAS 3-22761
GAS SIDE HEAT TRANSFER - 2-D FLOW

DATE
CHART NO. 19

TURNER HEAT TRANSFER DISTRIBUTION
TASK I PREDICTION

M_2 = 0.75
Re_2 = 1.0×10^6

♦ Tu = 5.9%
⊡ Tu = 2.2%
\+ Tu = 0.4%
——— TASK I PREDICTION

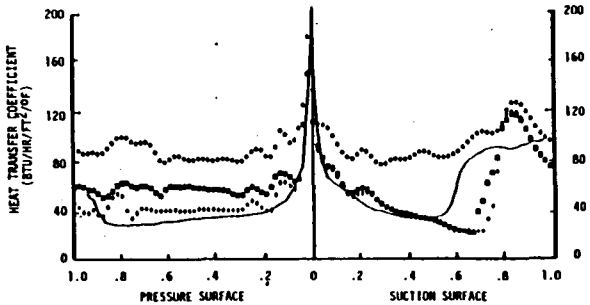

AXIAL CHORD - X/CX

Detroit Diesel Allison
Division of General Motors Corporation
Indianapolis, Indiana

NAS 3-22761
GAS SIDE HEAT TRANSFER - 2-D FLOW

DATE
CHART NO. 20

TURNER HEAT TRANSFER DISTRIBUTION
TASK III PREDICTIONS

M_2 = 0.75
Re_2 = 1.0×10^6

Tu(%)	DATA	TASK III PREDICTION
5.9	♦	—·—·—
2.2	⊡	- - - - -
0.4	+	———

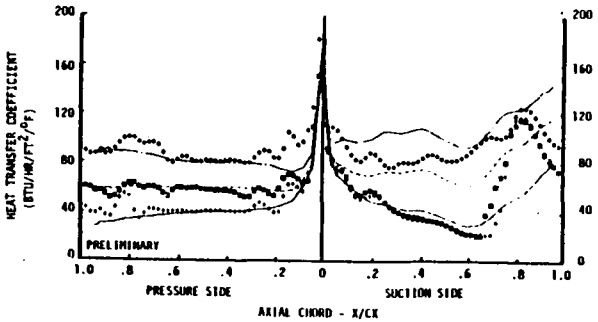

AXIAL CHORD - X/CX

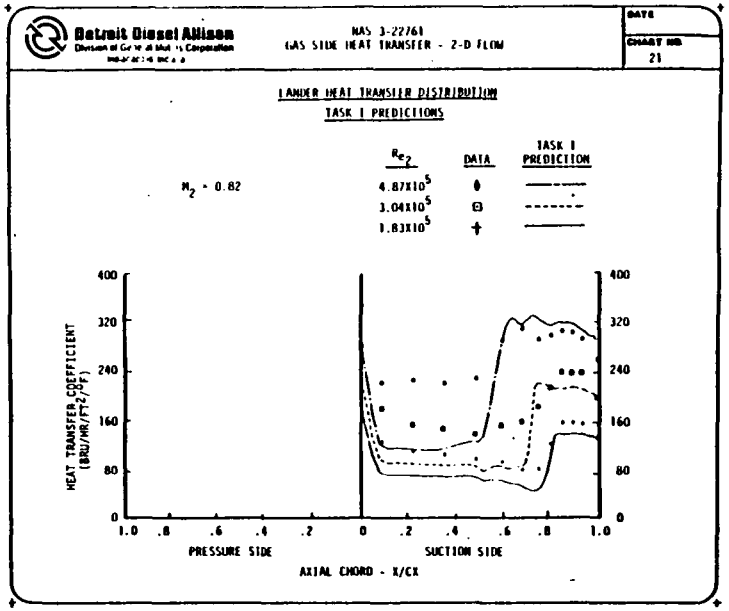
Detroit Diesel Allison
NAS 3-22761
GAS SIDE HEAT TRANSFER - 2-D FLOW
DATE
CHART NO
21
LANDER HEAT TRANSFER DISTRIBUTION
TASK I PREDICTIONS
M_2 = 0.82
Re_2
DATA
TASK I PREDICTION
4.87X10^5
3.04X10^5
1.83X10^5
HEAT TRANSFER COEFFICIENT (BTU/HR/FT2/°F)
400
320
240
160
80
0
1.0 .8 .6 .4 .2 0 .2 .4 .6 .8 1.0
PRESSURE SIDE
SUCTION SIDE
AXIAL CHORD - X/CX

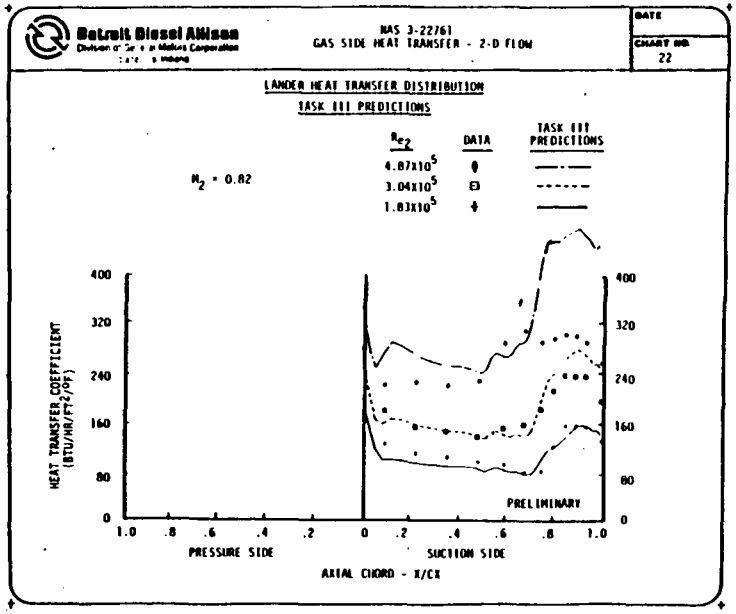
Detroit Diesel Allison
NAS 3-22761
GAS SIDE HEAT TRANSFER - 2-D FLOW
DATE
CHART NO
22
LANDER HEAT TRANSFER DISTRIBUTION
TASK III PREDICTIONS
M_2 = 0.82
Re_2
DATA
TASK III PREDICTIONS
4.87X10^5
3.04X10^5
1.83X10^5
HEAT TRANSFER COEFFICIENT (BTU/HR/FT2/°F)
400
320
240
160
80
0
1.0 .8 .6 .4 .2 0 .2 .4 .6 .8 1.0
PRESSURE SIDE
SUCTION SIDE
AXIAL CHORD - X/CX
PRELIMINARY